ORIGINAL RESEARCH

Oxidative stress contributes to cobalt oxide nanoparticles-induced cytotoxicity and DNA damage in human hepatocarcinoma cells

Saud Alarifi[1]
Daoud Ali[1]
Al Omar Suliman Y[2]
Maqusood Ahamed[3]
Maqsood A Siddiqui[2]
Abdulaziz A Al-Khedhairy[2]

[1]Cell and Molecular Laboratory, Department of Zoology, Faculty of Science, King Saud University, Riyadh, Saudi Arabia; [2]Faculty of Science, Department of Zoology, King Saud University, Riyadh, Saudi Arabia; [3]King Abdullah Institute for Nanotechnology, King Saud University, Riyadh, Saudi Arabia

Correspondence: Daoud Ali
Cell and Molecular Laboratory, Department of Zoology, Faculty of Science, King Saud University, Box 2455, Riyadh 11451, Saudi Arabia
Tel +966 5589 04621
Email daudali.ksu12@yahoo.com

Background: Cobalt oxide nanoparticles (Co_3O_4NPs) are increasingly recognized for their utility in biological applications, magnetic resonance imaging, and drug delivery. However, little is known about the toxicity of Co_3O_4NPs in human cells.

Methods: We investigated the possible mechanisms of genotoxicity induced by Co_3O_4NPs in human hepatocarcinoma (HepG2) cells. Cell viability, reactive oxygen species (ROS), glutathione, thiobarbituric acid reactive substance, apoptosis, and DNA damage were assessed in HepG2 cells after Co_3O_4NPs and Co^{2+} exposure.

Results: Co_3O_4NPs elicited a significant ($P < 0.01$) reduction in glutathione with a concomitant increase in lipid hydroperoxide, ROS generation, superoxide dismutase, and catalase activity after 24- and 48-hour exposure. Co_3O_4NPs had a mild cytotoxic effect in HepG2 cells; however, it induced ROS and oxidative stress, leading to DNA damage, a probable mechanism of genotoxicity. The comet assay showed a statistically significant ($P < 0.01$) dose- and time-related increase in DNA damage for Co_3O_4NPs, whereas Co^{2+} induced less change than Co_3O_4NPs but significantly more than control.

Conclusion: Our results demonstrated that Co_3O_4NPs induced cytotoxicity and genotoxicity in HepG2 cells through ROS and oxidative stress.

Keywords: cobalt oxide nanoparticles, HepG2 cells, cytotoxicity, oxidative stress, DNA damage

The use of nanotechnology has seen an exponential growth in the areas of health care, consumer products, clothes, electronics, and sporting goods.[1] This is due to the unique properties of nanomaterials (eg, chemical, mechanical, optical, magnetic, and biological), which make them desirable for commercial and medical applications.[2,3] According to a recent survey, the number of nanotechnology-based consumer products available in the world market has crossed the 1000 mark.[4] Thus, it is essential to assess the health hazards of nanomaterials in humans and other species.[2] Metal nanoparticles exhibit unique properties in terms of optical, magnetic, and electrical activity.[5] One of the most interesting chemical elements used as nanoparticles for biomedical applications is cobalt oxide nanoparticles (Co_3O_4NPs).

Occupational exposure of cobalt can lead to various lung diseases, such as interstitial pneumonitis, fibrosis, and asthma.[6] De Boeck et al[7] reported the genotoxic potential of cobalt nanoparticles in humans. A synergistic effect of cobalt and tungsten carbide enhanced production of reactive oxygen species (ROS) and induced DNA fragmentation.[8] In view of their possible risk for human health as nanotechnology products, the cytotoxic and genotoxic effects Co_3O_4NPs are of concern.

189

ROS is an important factor in the apoptosis process as well as in DNA damage,[9] oxidative stress-induced damage, and other cellular processes. However, the mechanisms involved in the toxicity of commercially important Co_3O_4NPs are poorly understood. Human hepatocarcinoma (HepG2) cells have been used as a surrogate for human hepatocytes and have found application in the study of nanoparticle cytotoxicity.[10] Subsequently, measurement of ROS with 2,7-dichlorfluorescein-diacetate (DCFH-DA) was carried out to determine whether ROS generation could be a possible mechanism in the observed cytotoxicity of Co_3O_4NPs. In the presence of DNA damage or cellular stress, p53 protein triggers cell-cycle arrest to provide time for the damage to be repaired or for self-mediated apoptosis.[11] Recent studies have shown that Co_3O_4NPs releases cobalt ions (Co^{2+}) in the aqueous state. Therefore, we also investigated whether Co_3O_4NPs induce a cellular response in HepG2 cells, and if so, whether they produce toxicity by releasing soluble Co^{2+} or by exerting a toxic effect unique to Co_3O_4NPs.

The present investigations were carried out to study the underlying mechanisms of cytotoxicity and genotoxicity induced by Co_3O_4NPs in human hepatoma cells through ROS generation and oxidative stress.

Materials and methods
Chemicals and reagents
Fetal bovine serum, penicillin–streptomycin, and Dulbeco's Modified Eagle's Medium: Nutrient Mixture F-12 (DMEM/F-12) were purchased from Invitrogen (Carlsbad, CA, USA). Co_3O_4NPs, glutathione (GSH), 5, 5-dithio-bis-(2-nitrobenzoic acid), MTT [3-(4,5-dimethylthiazol-2-yl)-2,5-diphenyltetrazoliumbromide], Dichlorofluorescin diacetate (DCFH-DA), and propidium iodide were obtained from Sigma-Aldrich (St Louis, MO, USA). Cobalt chloride and all other chemicals used were of high purity and available from commercial sources.

Co_3O_4 nanoparticle preparation and characterization
Co_3O_4NPs were suspended in Milli-Q water (EMD Millipore, Billerica, MA, USA) at a concentration of 1 mg/mL. Stock suspension was probe sonicated at 40 W for 15 minutes. The optical absorption of the Co_3O_4NPs suspension was measured using a double beam ultraviolet–visible (UV-Vis) spectrum (Varian-Cary-300 UV-Vis Spectrophotometer, BioTech, MD, USA) in the wavelength range of 200–800 nm

at room temperature. The average hydrodynamic size of the Co_3O_4NPs was measured by dynamic light scattering (DLS) (Nano-Zeta Sizer-HT; Malvern Instruments, Worecestershire, UK) following the procedure of Murdock et al.[12]

Samples for transmission electron microscopy (TEM) analysis were prepared by drop coating Co_3O_4NP solution on carbon-coated copper TEM grids. The films on the TEM grids were allowed to dry prior to measurement. TEM measurements were performed on a JEOL model 2100F (JEOL, Tokyo, Japan) operated at an accelerating voltage at 200 kV.

Cell culture and exposure of Co_3O_4NPs
HepG2 (passage no 28) was procured from the American Type Culture Collection (Accession no HB-8065; Rockville, MD, USA) and was preserved and subcultured up to passage no 40 in the laboratory. The subcultures were used to determine cell viability against Co_3O_4NPs and Co^{2+} exposure. Cells were cultured in DMEM/F-12 medium supplemented with 10% fetal bovine serum and 100 U/mL penicillin–streptomycin at 5% CO_2 and 37°C. At 85% confluence, cells were harvested by using 0.25% trypsin and were subcultured into 75 cm^2 flasks, 6-well plates, or 96-well plates according to the type of experiment. Cells were allowed to attach to the surface for 24 hours prior to treatment. Co_3O_4NPs were suspended in cell culture medium and diluted to appropriate concentrations (0, 5, 10, 15, and 25 µg/mL). The appropriate dilutions of Co_3O_4NPs were then sonicated in a sonicator bath at room temperature for 10 minutes at 40 W to avoid particle agglomeration before exposure to cells. Cells not exposed to Co_3O_4NPs served as the control in each experiment.

Analysis of dissolution of Co_3O_4NPs
Dissolution of Co_3O_4NPs and the effects from exposure to cells were analyzed to determine whether Co^{2+} released from Co_3O_4NP suspension may play a role in cellular toxicity. The released Co^{2+} concentrations were measured in all the culture media collected from the Co_3O_4NP treatment. Culture media were taken from the Co_3O_4NP-treated cells immediately at the end of exposure and centrifuged at 30,000 g for 30 minutes. After centrifugation, the released Co^{2+} concentrations in the supernatants were detected by flame atomic absorption spectroscopy (GBC Avanta Ver 2.0; Sigma-Aldrich).

To compare the toxic effects of released Co^{2+} with Co_3O_4NPs, another exposure regime with soluble Co^{2+} was

performed. The Co_3O_4NPs suspension was replaced by Co^{2+} solution (10, 15, and 25 µg/mL), which was dosed by adding the required mass of cobalt chloride (97.0%–100%, BDH Chemicals, Radnor, PA, USA) to the culture medium.

Cell morphology

Morphology of the HepG2 cells was observed after exposure to different concentrations of Co_3O_4NPs for 24 and 48 hours by using a Leica DMIL phase-contrast microscope (Leica Microsystems, Wetzlar, Germany).

Mitochondrial function

The MTT assay was used to investigate mitochondrial function as described by Mossman.[13] Briefly, 1×10^4 cells/well were seeded in 96-well plates and exposed to different concentrations of Co_3O_4NPs and Co^{2+} for 24 and 48 hours. At the end of exposure, culture media was replaced with new media containing MTT solution (0.5 mg/mL) and incubated for 4 hours at 37°C. As a result, formazan crystal was formed, which was dissolved in Dimethyl sulfoxide (DMSO). The plates were kept on a shaker for 10 minutes at room temperature and then analyzed at 530 nm with a multiwell microplate reader (Omega Fluostar, BMG Labtech GmbH, Allmendgruen, Germany). Untreated sets were also run under identical conditions and served as control.

Lactate dehydrogenase leakage assay

The release of cytoplasmic lactate dehydrogenase enzyme (LDH) into the culture medium was determined following Wroblewski and LaDue.[14] HepG2 cells were treated with different concentrations of Co_3O_4NPs and Co^{2+} for 24 and 48 hours. After exposure, 100 µL samples from the centrifuged culture media were collected. The LDH activity was assayed in 3.0 mL of reaction mixture with 100 µL of pyruvic acid (2.5 mg/mL phosphate buffer) and 100 µL of reduced nicotinamide adenine dinucleotide (NADH) (2.5 mg/mL phosphate buffer); the rest of the volume was adjusted with phosphate buffer (0.1 M, pH 7.4). The rate of NADH oxidation was determined by following the decrease in absorbance at 340 nm for 3 minutes at 1-minute intervals at 25°C using a spectrophotometer (Varian-Cary 300 Bio).The amount of LDH released was expressed as LDH activity (IU/L) in culture media.

Measurement of intracellular ROS

We used fluorometric analysis and microscopic fluorescence imaging to study ROS generation in HepG2 cells after expo-

sure to different concentrations of Co_3O_4NPs and Co^{2+}.[15] For fluorometric analysis, cells (1×10^4 per well) were seeded in 96-well black bottom culture plates and allowed to adhere for 24 hours in a CO_2 incubator at 37°C. HepG2 cells were then exposed to 5, 10, and 15 µg/mL concentrations of Co_3O_4NPs and Co^{2+} for 24 and 48 hours. After exposure, cells were incubated with DCFH-DA (10 mM) as the fluorescence agent for 30 minutes at 37°C. The reaction mixture was aspirated and replaced by 200 µL of phosphate-buffered saline (PBS) in each well. The plates were kept on a shaker for 10 minutes at room temperature in the dark. Fluorescence intensity was measured with a multiwell microplate reader (Omega Fluostar) at an excitation wavelength of 485 nm and at an emission wavelength of 528 nm. Values were expressed as the percentage of fluorescence intensity relative to the control wells.

An upright fluorescence microscope equipped with a CCD cool camera (Nikon Eclipse 80i with Nikon DS-Ri1 12.7 megapixel camera; Nikon Corporation, Tokyo Japan) was used to analyze intracellular fluorescence of a second set of cells (5×10^4 per well) prepared as described above.

Oxidative stress biomarkers

Cells at a final density of ~6×10^6 in a 75 cm^2 culture flask were exposed to different concentrations of (5,10 and 15 µg/mL) of Co_3O_4NPs and (10 and 15 µg/mL) of Co^{2+} for 24 and 48 hours. After exposure, the cells were scraped and washed twice with chilled 1× PBS. The harvested cell pellets were lysed in cell lysis buffer (20 mM Tris-HCl [pH 7.5], 150 mM NaCl, 1 mM Na_2EDTA, 1% Triton, and 2.5 mM sodium pyrophosphate). The cells were centrifuged at 15,000 g for 10 minutes at 4°C, and the supernatant (cell extract) was maintained on ice until assayed for oxidative-stress biomarkers. Protein content was measured by the method of Bradford,[16] using bovine serum albumin as the standard.

Lipid peroxidation assay

The extent of membrane lipid peroxidation (LPO) was estimated by measuring the formation of malondialdehyde (MDA), one of the products of membrane LPO, using the method of Ohkawa et al.[17] A mixture of 0.1 mL cell extract and 1.9 mL of 0.1 M sodium phosphate buffer (pH 7.4) was incubated at 37°C for 1 hour. After precipitation with 5% trichloroacetic acid, the incubation mixture was centrifuged at 2300 g for 15 minutes at room temperature. One milliliter of 1% thiobarbituric was added to the supernatant, which was then placed in boiling water for 15 minutes. After cooling to room temperature, absorbance of the mixture at 532 nm

was expressed in nmol MDA/hour/mg protein using a molar extinction coefficient of 1.56×10^5/M/cm.

GSH estimation

GSH level was quantified by using Ellman's reagent.[18] The assay mixture contained phosphate buffer, DTNB, and cell extract. The reaction was monitored at 412 nm, and the amount of GSH was expressed in terms of nmol GSH/mg protein.

Measurement of superoxide dismutase

Superoxide dismutase (SOD) activity was estimated using a method described by Kakkar et al.[19] The assay mixture contained sodium pyrophosphate buffer, nitroblue tetrazolium, phenazine methosulphate, reduced nicotinamide adenine dinucleotide, and the required volume of cell extract. One unit of SOD enzyme activity is defined as the amount of enzyme required for inhibiting chromogen production (optical density at 560 nm) by 50% in 1 minute under assay conditions and is expressed as specific activity in units/minute/mg protein.

Measurement of catalase level

Catalase (CAT) activity was measured by following its ability to split hydrogen peroxide (H_2O_2) within 1 minute of incubation time. The reaction was then stopped by adding dichromate/acetic acid reagent, and the remaining H_2O_2 was determined by measuring chromic acetate at 570 nm. Chromic acetate is formed by the reduction of dichromate/acetic acid in the presence of H_2O_2, as described by Sinha.[20] CAT activity was expressed as μM H_2O_2 decomposition/minute/mg protein.

Caspase-3 assay

The activity of caspase-3 was determined from the cleavage of the caspase-3 substrate (N-acetyl-DEVD-p-nitroaniline). p-Nitroaniline was used as the standard. Cleavage of the substrate was monitored at 405 nm, and the specific activity was expressed as pM of the product (nitroaniline) per minute/mg protein.

DAPI staining for chromosome condensation

Chromosome condensation in HepG2 cells due to Co_3O_4NPs and Co^{2+} was observed by DAPI staining according to the method of Dhar-Mascareno et al.[21] Cells were placed in eight chamber slides, which were incubated in the DAPI solution for 10 minutes

in the dark at 37°C. Images of the nucleus were captured by fluorescence microscopy (Nikon) at an excitation wavelength of 330 nm and an emission wavelength of 420 nm.

Determination of DNA strand breakage

Alkaline single cell gel electrophoresis was performed as a three-layer procedure[22] with slight modification.[23] In brief, 70,000 cells/well were seeded in a six-well plate. After 24 hours, cells were treated with different concentrations of Co_3O_4NPs and Co^{2+} for 24 and 48 hours. After treatment, the HepG2 cells were trypsinized and resuspended in DMEM, and the cell suspension was centrifuged at 1200 rpm at 4°C for 5 minutes. The cell pellet was then suspended in chilled PBS for the comet assay. Viability of cells was evaluated by the trypan blue exclusion method.[24] Samples showing cell viability higher than 84% were further processed for the comet assay. In brief, about 15 μL of cell suspension (~20,000 cells) was mixed with 85 μL of 0.5% low-melting-point agarose and layered on one end of a frosted plain glass slide, precoated with a layer of 200 μL normal agarose (1%). The sample was then covered with a third layer of 100 μL low-melting-point agarose. After solidification of the gel, the slides were immersed in lysing solution (2.5 M NaCl, 100 mM Na_2EDTA, 10 mM Tris [pH 10] with10% DMSO, and 1% Triton X-100 [added fresh]) overnight at 4°C. The slides were then placed in a horizontal gel electrophoresis unit. Fresh cold alkaline electrophoresis buffer (300 mM NaOH, 1 mM Na_2EDTA, and 0.2% DMSO), pH 13.5, was poured into the chamber and left for 20 minutes at 4°C for DNA unwinding and conversion of alkali-labile sites to single-strand breaks. Electrophoresis was carried out using the same solution at 4°C for 20 minutes at 15 V (0.8 V/cm) and 300 mA. The slides were neutralized gently with 0.4 M tris buffer at pH 7.5 and stained with 75 μL ethidium bromide (20 μg/mL). For the positive control, the HepG2 cells were treated with 100 μM H_2O_2 for 10 minutes at 4°C. Two slides were prepared from each well (per concentration), and 50 cells per slide (100 cells per concentration) were scored randomly and analyzed using an image analysis system (Komet-5.0; Kinetic Imaging, Liverpool, UK) attached to fluorescence microscope (DMLB, Leica, Germany) equipped with appropriate filters. The parameters, percent tail DNA (% tail DNA = 100 − % head DNA) and olive tail moment, were selected for quantification of DNA damage in HepG2 cells as determined by the software (Komet-5.0; Kinetic Imaging, Liverpool, UK).
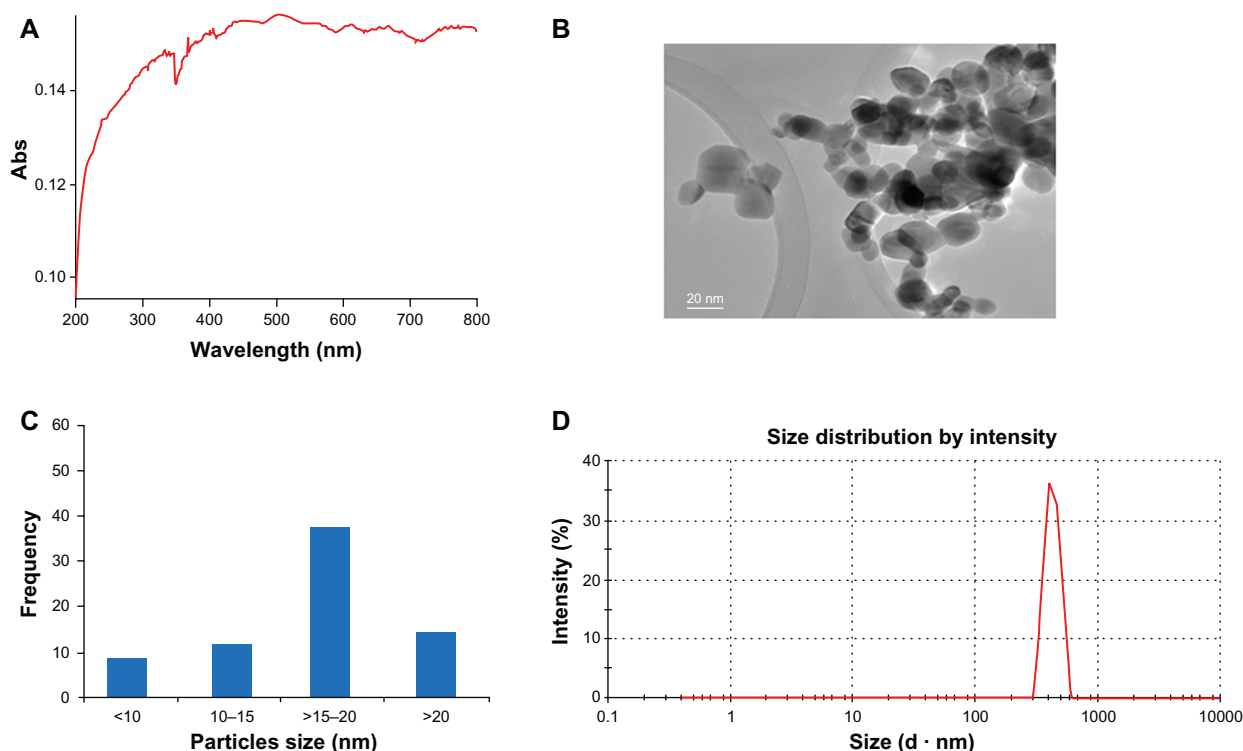
Figure 1 Characterization of Co$_3$O$_4$NPs. (**A**) UV-visible spectrum of Co$_3$O$_4$NPs. (**B**) TEM image. (**C**) Size distribution histogram generated by using a TEM image. (**D**) Size distribution and zeta potential of Co$_3$O$_4$NPs were determined using dynamic light scattering.
Note: Analysis was performed from the stock solution.
Abbreviations: Abs, absorbance; Co$_3$O$_4$NPs, cobalt oxide nanoparticles; TEM, transmission electron microscopy.

Statistical analysis

At least three independent experiments were carried out in duplicate for each experiment. Data were expressed as mean (±standard error) and analyzed by one-way analysis of variance. $P < 0.01$ was considered statistically significant.

Results

Physicochemical characterization of Co$_3$O$_4$NPs

Results from the UV-Vis spectrophotometer showed an absorption band (Figure 1A). A typical TEM image of the

Co$_3$O$_4$NPs (Figure 1B) showed that the majority of particles had a polygonal shape with smooth surfaces. The average particle diameter of approximately 21 nm was calculated from measuring over 100 particles in random fields of TEM view (Figure 1C). The average hydrodynamic size and zeta potential of the Co$_3$O$_4$NPs in water determined by DLS were 264.8 nm and −15.3 mV, respectively (Figure 1D).

Effect of Co$_3$O$_4$NPs on morphological changes and cytotoxicity

Figure 2 shows the comparative morphology of untreated and Co$_3$O$_4$NPs-treated HepG2 cells. Morphological changes in cells were visible after 10 µg/mL Co$_3$O$_4$NPs exposure in 24 hours. Cells treated with 25 µg/mL Co$_3$O$_4$NPs after 48 hours changed to a spherical shape and detached from the surface (Figure 1B). The morphology of the HepG2 cells exposed to Co$_3$O$_4$NPs supported the results showing membrane damage and cytotoxicity.

We examined the mitochondrial function (MTT reduction) and membrane damage (LDH leakage) as cytotoxicity end points. MTT results demonstrated a concentration and time-dependent cytotoxicity after exposure to Co$_3$O$_4$NPs
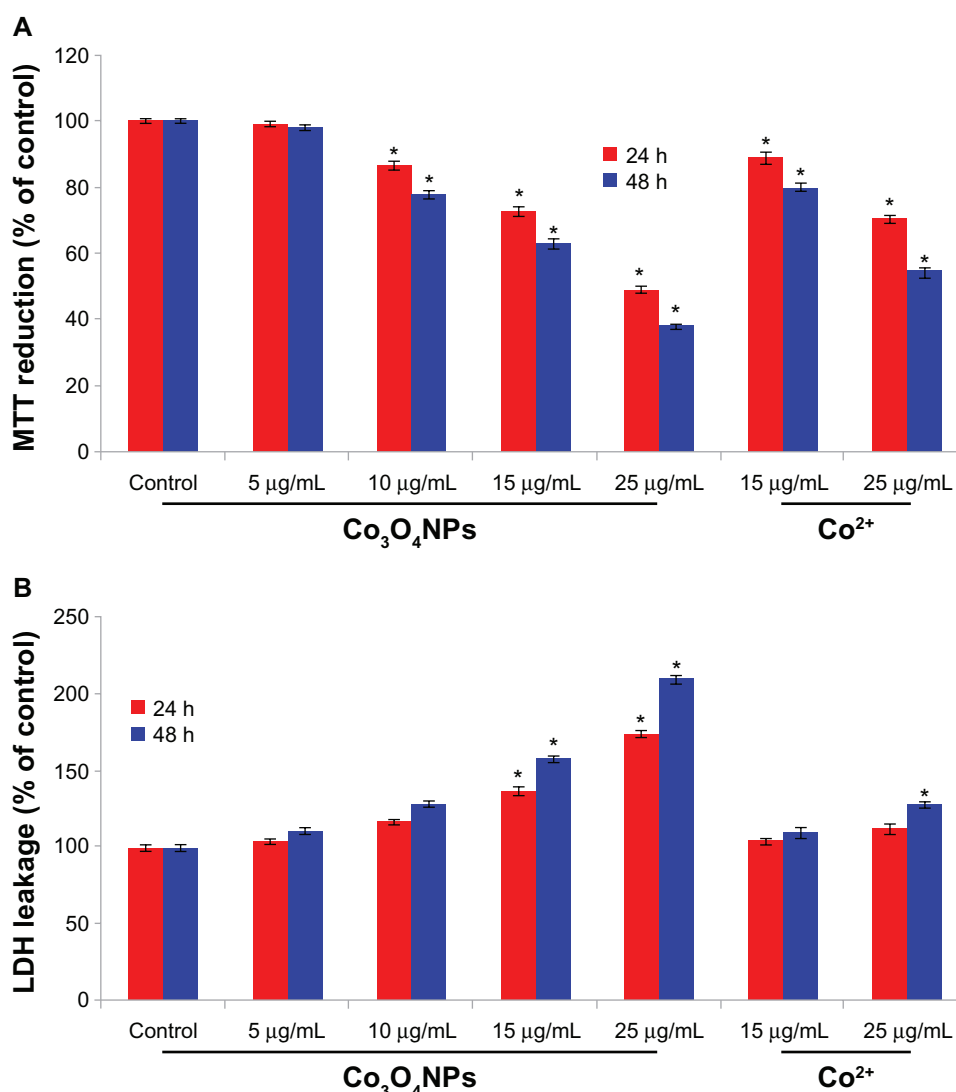

Figure 2 Morphology of HepG2 cells. (**A**) Control; (**B**) 25 µg/mL of Co$_3$O$_4$NPs treated for 48 hours.
Note: Magnification 200×.
Abbreviations: HepG2, human hepatocarcinoma; Co$_3$O$_4$NPs, cobalt oxide nanoparticles.

Figure 3 Cytotoxicity of Co_3O_4NPs and Co^{2+} in HepG2 cells for 24 hours and 48 hours. (**A**) MTT reduction; (**B**) LDH leakage.
Notes: Each value represents the mean ± standard error of three experiments, performed in duplicate. *$P < 0.01$ vs control.
Abbreviations: Co_3O_4NPs, cobalt oxide nanoparticles; Co^{2+}, cobalt ions; HepG2, human hepatocarcinoma; MTT, 3-(4,5-dimethylthiazol-2-yl)-2,5-diphenyltetrazoliumbromide; LDH, lactate dehydrogenase enzyme.

in HepG2 cells (Figure 3A). MTT reduction observed after 24 hours of exposure at concentrations of 5, 10, 15, and 25 μg/mL was 1.6%, 10.0%, 30.7%, and 46.0%, respectively, with a further reduction to 3.4%, 24.61%, 36%, and 62% after 48 hours exposure. Co_3O_4NPs was also found to induce LDH leakage in a concentration- and time-dependent manner (Figure 3B).

Co_3O_4NPs induced ROS generation and oxidative stress

The ability of Co_3O_4NPs to induce oxidative stress was evaluated by measuring the levels of ROS, LPO, GSH,

SOD, and catalase in HepG2 cells. Results showed that Co_3O_4NPs induced intracellular ROS generation in a dose- and time-dependent manner (Figure 4). Co_3O_4NPs-induced oxidative stress was further evidenced by depletion of GSH and induction of LPO, SOD, and catalase with concentration and time of Co_3O_4NPs exposure (Figure 5A–D).

Induction of caspase-3 activity and chromosome condensation by Co_3O_4NPs

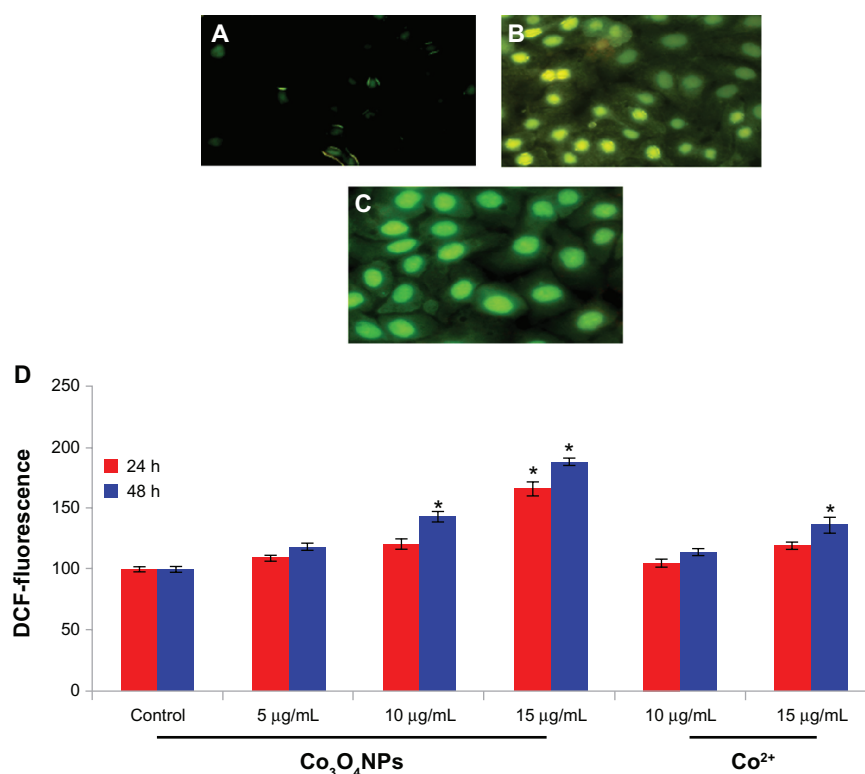Caspase-3, which plays a key role in the apoptotic pathway of cells, was induced following treatment with Co_3O_4NPs

Figure 4 Representative microphotographs showing Co_3O_4NP- and Co^{2+}-induced ROS generation in HepG2 cells. Images were snapped with Nikon phase contrast with a fluorescence microscope. (**A**) Control; (**B**) 15 µg/mL of Co^{2+}; (**C**) 15 µg/mL of Co_3O_4NPs; (**D**) percentage change in ROS generation after 24 and 48 hours exposure to various concentrations of Co_3O_4NPs and Co^{2+} in HepG2 cells.
Notes: Each value represents the mean ± standard error of three experiments, performed in duplicate. *$P < 0.01$ vs control.
Abbreviations: Co_3O_4NPs, cobalt oxide nanoparticles; Co^{2+}, cobalt ions; ROS, reactive oxygen species; HepG2, human hepatocarcinoma.

(Figure 6D). When cells were treated with 5, 10, and 15 µg/mL concentrations of Co_3O_4NPs for 24 and 48 hours, caspase-3 activity increased in a concentration- and time-dependent manner. In addition to the caspase-3 activity, chromatin condensation was also evaluated by DAPI staining. When cells were treated with the above concentrations of Co_3O_4NPs for 24 hours, chromatin condensation was observed in the treated group (Figure 6A–C). Caspase-3 activation and chromatin condensation in HepG2 cells suggest that Co_3O_4NPs caused cell death by an apoptotic process.

DNA damage by Co_3O_4NPs

DNA damage was measured as percentage tail DNA and olive tail moment in the control as well as exposed cells. During electrophoresis, cell DNA was observed to migrate more rapidly toward the anode at the highest concentration compared to the lowest concentration. The cells exposed to different concentrations of Co_3O_4NPs exhibited significantly ($P > 0.01$) higher DNA damage than those of the control groups. A gradual nonlinear

increase in DNA damage was observed in cells as dose and time of Co_3O_4NPs exposure increased. The highest DNA damage was recorded at 15 µg/mL Co_3O_4NPs in HepG2 cells (Figure 7).

Dissolution of Co_3O_4NPs into Co^{2+} and effects of soluble Co^{2+} on cytotoxicity, oxidative stress, apoptosis markers, and DNA damage

To determine whether our observed cytotoxicity, oxidative stress, apoptosis and DNA damage could be attributed to the released Co^{2+}, we analyzed the level of Co^{2+} released from Co_3O_4NPs and tested the effect of Co^{2+} concentration in HepG2 cells. The highest released Co^{2+} concentration in the Co_3O_4NP suspension following exposure was 0.86 ± 0.28 µg/mL in the 25 µg/mL Co_3O_4NP suspension. The released Co^{2+} concentrations in 5, 10, and 15 µg/mL Co_3O_4NPs treatments were 0.14 ± 0.06, 0.39 ± 0.23, and 0.48 ± 0.337 µg/mL, respectively. Our data on the dissolution of Co_3O_4NPs in the aqueous state are in agreement with other recent studies (Papis et al[25]). We examined

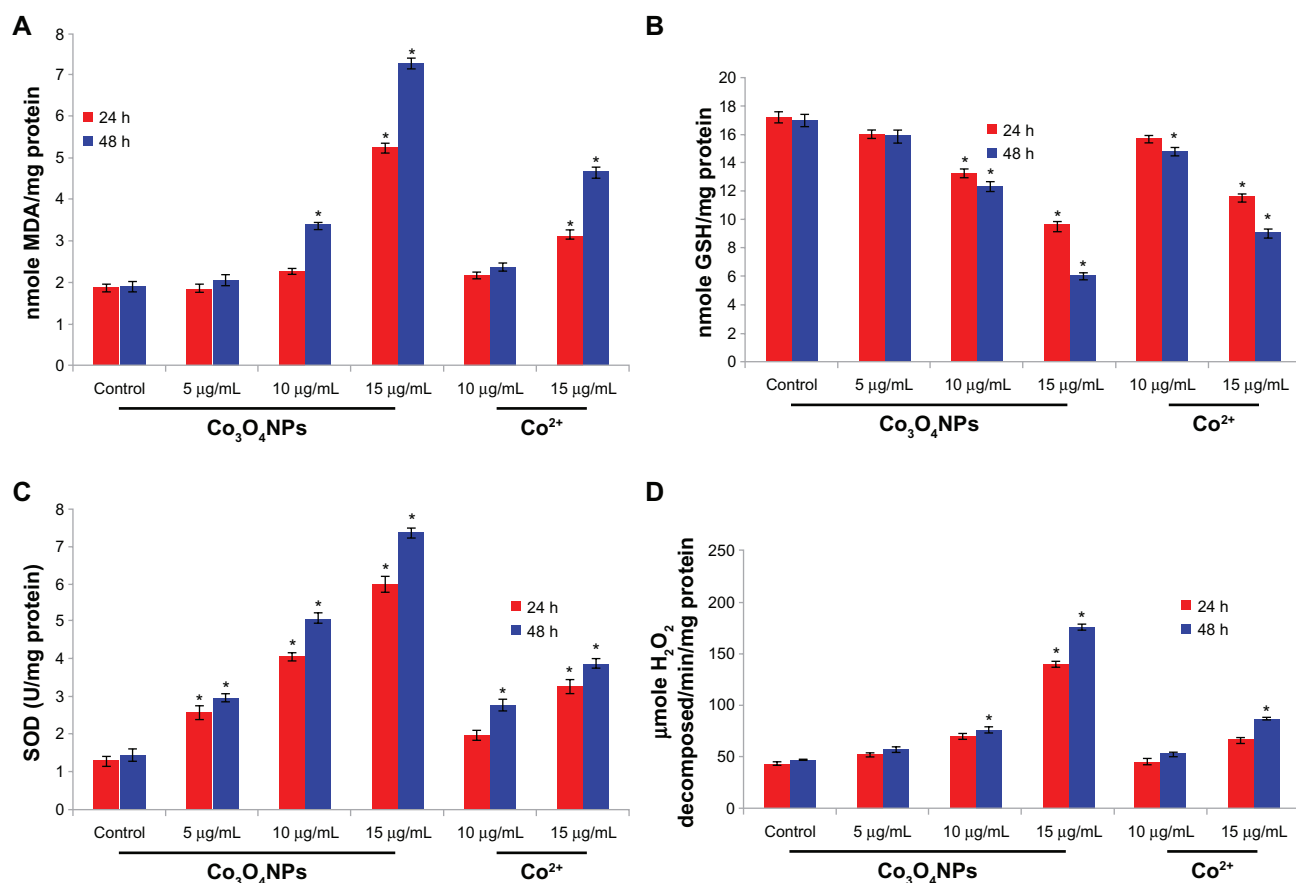**Figure 5** (**A**) Levels of lipid peroxides; (**B**) GSH; (**C**) SOD; (**D**) catalase in HepG2 cells after exposure of Co_3O_4NPs and Co^{2+} for 24 and 48 hours.
Notes: Each value represents the mean ± standard error of three experiments, performed in duplicate. *$P < 0.01$ vs control.
Abbreviations: GSH, glutathione; SOD, superoxide dismutase; HepG2, human hepatocarcinoma; Co_3O_4NPs, cobalt oxide nanoparticles; Co^{2+}, cobaltions; MDA, malondialdehyde.

the toxic effect of 10, 15, and 25 µg/mL of soluble Co^{2+} in HepG2 cells and found that Co^{2+} exerted cytotoxicity (MTT reduction and LDH leakage), oxidative stress (ROS, LPO, GSH, CAT, and SOD), apoptosis (caspase-3 and chromatin condensation), and DNA damage, but effects were less significant compared to similar concentrations of Co_3O_4NPs, as shown in Figures 2–7.

Discussion

Cobalt-based NPs are used in different types of technological products, such as sensors, catalysts, and energy storage devices.[26] HepG2 cells retain the function of fully differentiated primary hepatocytes and are widely used as a model system for hepatotoxicity studies.[27] Recent studies showed that Co^{2+} is released from Co_3O_4NPs when they are suspended in the aqueous state.[28] In the present study, we examined the dissolution of Co_3O_4NPs in an aqueous suspension and their toxicity to HepG2 cells. Our results agree with the findings of Colognato et al[29] in which they reported that Co_3O_4NPs liberate Co^{2+} in the aqueous state, but the level of Co^{2+} was

insufficient to induce cell toxicity. We used MTT and LDH assays to evaluate the cytotoxicity of Co_3O_4NPs in order to obtain more reliable data. MTT and LDH assays are frequently utilized to determine the cytotoxicity of nanoparticles in cell culture systems.[30,31] Both assays demonstrated that Co_3O_4NPs produce significant cytotoxicity to HepG2 cells in a dose- and time-dependent manner.

Oxidative stress has been suggested as playing an important role in the mechanism of toxicity for a number of nanoparticles through either the excessive generation of ROS or depletion of cellular antioxidant capacity.[32] ROS typically include the superoxide radical (O^{2-}), H_2O_2, and the hydroxyl radical ($\cdot OH$), all of which cause damage to cellular components, including DNA damage, and ultimately apoptotic cell death.[33] In the present study, Co_3O_4NPs significantly altered oxidant/antioxidant levels in HepG2 cells. Generation of ROS, LPO, SOD, and catalase activities increased, while the antioxidant molecule GSH significantly declined in Co_3O_4NP-exposed cells. GSH, a ubiquitous and abundant cellular antioxidant tripeptide, has been shown to
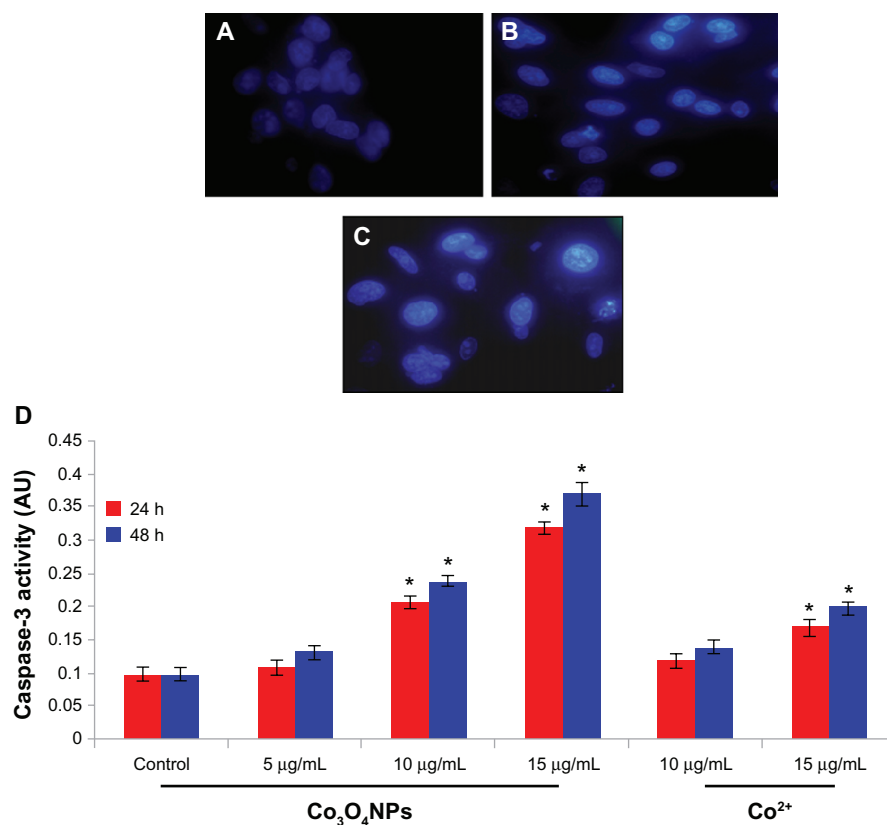
Figure 6 Increase of chromosome condensation and caspase-3 activity in HepG2 cells after exposure of Co_3O_4NPs and Co^{2+} for 24 and 48 hours. (**A**) Control; (**B**) exposed to 15 μg/mL Co^{2+}; (**C**) exposed to 15 μg/mL Co_3O_4NPs; (**D**) caspase-3 activity.
Notes: Each value represents the mean ± standard error of three experiments. *$P < 0.01$ vs control.
Abbreviations: HepG2, human hepatocarcinoma; Co_3O_4NPs, cobalt oxide nanoparticles; Co^{2+}, cobalt ions.

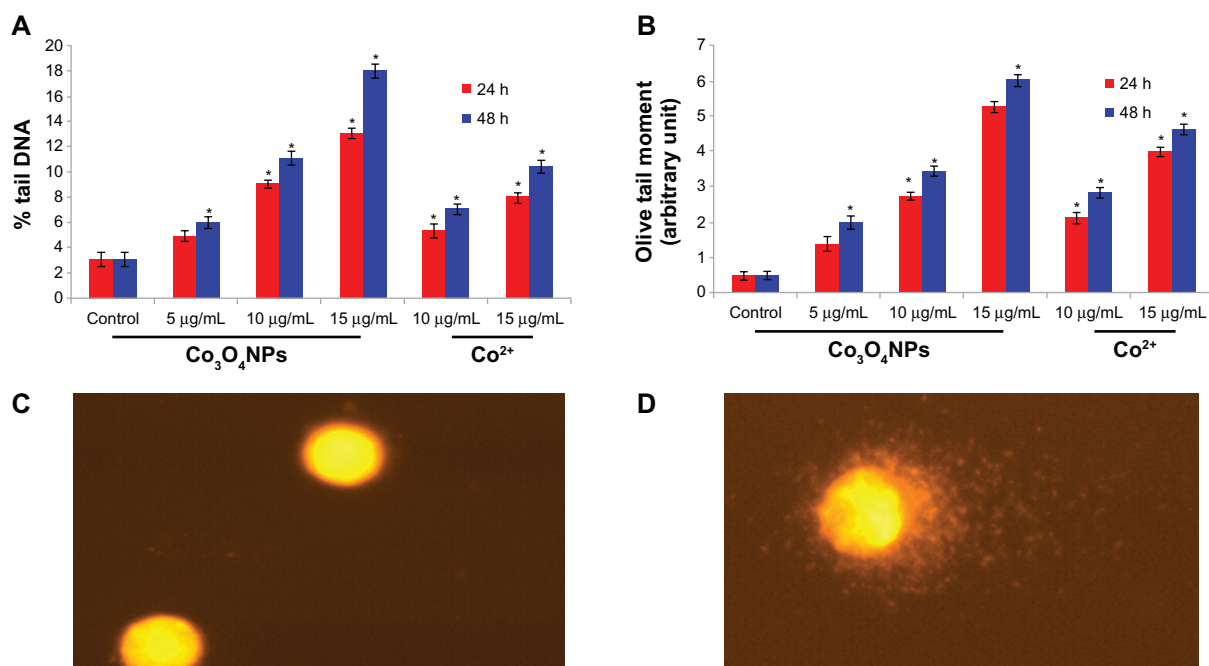**Figure 7** DNA damage in HepG2 cells after 24 hours and 48 hours of exposure to different concentrations of Co_3O_4NPs and Co^{2+}. (**A**) Percentage tail DNA; (**B**) olive tail moment (arbitrary unit); (**C**) control cell; (**D**) exposed cell.
Notes: Each value represents the mean ± standard error of three experiments, performed in duplicate. *$P < 0.01$ vs control.
Abbreviations: HepG2, human hepatocarcinoma; Co_3O_4NPs, cobalt oxide nanoparticles; Co^{2+}, cobalt ions.

be strongly depleted in response to nanoparticle exposure.[34] SOD is specialized to convert highly superoxide radicals to less toxic H_2O_2. Higher production of intracellular ROS and membrane LPO in Co_3O_4NP-exposed cells along with depletion of antioxidant components suggest that oxidative stress might be the primary mechanism for toxicity of Co_3O_4NPs in HepG2 cells. In the present study, ROS and MDA levels were significantly higher, while the antioxidant GSH level was significantly lower in HepG2 cells exposed to Co_3O_4NPs. ROS, such as O^{2-}, $OH\bullet$ and H_2O_2 elicit a variety of physiological and cellular events, including inflammation, DNA damage, and apoptosis.[35] Caspases are known to play a vital role in both initiation and execution of apoptosis, and in the present study we observed that caspase-3 levels increased in HepG2 cells after Co_3O_4NPs exposure. Caspase-3 has been reported as being essential for cellular DNA damage and apoptosis.[36]

Information on the effects of environmental exposure of Co_3O_4NPs to humans and potential health impacts is still lacking. The cell membrane offers an excellent barrier for most ions, and cobalt, in the ionic form, has been shown to have a lower efficiency in cell uptake.[29] In our experiments, Co_3O_4NPs induced a concentration- and time-dependent impairment of DNA damage, although Co^{2+} showed less genotoxicity. Our results are similar to those showing that Co_3O_4NPs induce genotoxicity in human leukocytes.[37] Cobalt-enhanced ROS formation oxidize proteins[38] and cause oxidative DNA damage but show a neuroprotective effect on hypoxia-induced oxidative stress.[39]

DNA damage, apoptosis, and oxidative stress markers raise concern about the safety associated with applications of Co_3O_4NPs in consumer products. However, more in vivo studies are needed to fully understand the mechanism of Co_3O_4NP toxicity.

Acknowledgment

Disclosure

The authors report no conflicts of interest in this work.

References

1. Singh N, Manshian B, Jenkins GJ, et al. Nano genotoxicology: the DNA damaging potential of engineered nanomaterials. *Biomaterials*. 2009;30:3891–3914.
2. Oberdorster G, Oberdorster E, Oberdorster J. Nanotoxicology: an emerging discipline evolving from studies of ultrafine particles. *Environ Health Persp*. 2005;113:823–839.
3. Jin CY, Zhu BS, Wang XF, Lu QH. Cytotoxicity of titanium dioxide nanoparticles in mouse fibroblast cells. *Chem Res Toxicol*. 2008;21: 1871–1877.
4. PEN 2009. Project of the Emerging Nanotechnologies (PEN). [webpage on the Internet]. Available at: http://www.nanotechproject.org.
5. Mandal S, Phadtare S, Sastry M. Interfacing biology with nanoparticles. *Curr App Phys*. 2005;5:118–127.
6. ATSDR. Public health assessments completed. Agency for Toxic Substances and Disease Registry (ATSDR), Department of Health and Human Services (HHS). *Notice Fed Regist*. 1999;64:4422–4423.
7. De Boeck M, Lombaert N, De Backer S, Finsy R, Lison D, Kirsch-Volders M. In vitro genotoxic effects of different combinations of cobalt and metallic carbide particles. *Mutagenesis*. 2003;18: 177–186.
8. Lison D, Carbonnelle P, Mollo L, Lauwerys R, Fubini B. Physicochemical mechanism of the interaction between cobalt metal and carbide particles to generate toxic activated oxygen species. *Chem Res Toxicol*. 1995;8:600–606.
9. Patlolla A, Patlolla B, Tchounwou P. Evaluation of cell viability, DNA damage, and cell death in normal human dermal fibroblast cells induced by functionalized multi walled carbon nanotube. *Mo Cell Biochem*. 2010;338:225–232.
10. Jan E, Byrne SJ, Cuddihy M, et al. High-content screening as a universal tool for fingerprinting of cytotoxicity of nanoparticles. *ACS Nano*. 2008;2:928–938.
11. Nel A, Xia T, Madler L, Li N. Toxic potential of materials at the nanolevel. *Science*. 2006;311:622–627.
12. Murdock RC, Braydich-Stolle L, Schrand AM, Schlager JJ, Hussain SM. Characterization of nanomaterial dispersion in solution prior to in vitro exposure using dynamic light scattering technique. *Toxicol Sci*. 2007;101:239–253.
13. Mossman T. Rapid colorimetric assay for cellular growth and survival: application to proliferation and cytotoxicity assays. *J Immunol Meth*. 1983;65:55–63.
14. Wroblewski F, LaDue JS. Lactate dehydrogenase activity in blood. *Pro of the Soc for Experim Biol and Med.* 1955;90:210–213.
15. Wang H, Joseph JA. Quantifying cellular oxidative stress by dichlorofluorescein assayusing microplate reader. *Free Radic Biol Med*. 1999;27:612–616.
16. Bradford MM. A rapid and sensitive method for the quantization of microgram quantities of protein utilizing the principle of protein-dye binding. *Anal Biochem*. 1976;72:248–254.
17. Ohkawa H, Ohishi N, Yagi K. Assay for lipid peroxides in animal tissues bythiobarbituric acid reaction. *Anal Biochem*. 1979;95: 351–358.
18. Ellman G. Tissue sulfhydryl groups. *Arch Biochem Biophys*. 1959;82: 70–77.
19. Kakkar PS, Das B, Viswanathan PN. A modified spectrophotometric assay of superoxide dismutase. *Ind J Biochem Biophys*. 1984;21: 130–132.
20. Sinha AK. Colorimetric assay of catalase. *Anal Biochem*. 1972;47: 389–394.
21. Dhar-Mascareno M, Carcamo JM, Golde DW. Hypoxia-reoxygenation-induced mitochondrial damage and apoptosis in human endothelial cells are inhibited by vitamin C. *Free Radic Bio Med*. 2005;38: 1311–1322.
22. Singh NP, McCoy MT, Tice RR, Schneider EL. A simple technique for quantization of low levels of DNA damage in individual cells. *Exp Cell Res*. 1988;175:184–191.
23. Ali D, Ray RS, Hans RK. UVA-induced cyotoxicity and DNA damaging potential of Benz (e) acephenanthrylene in human skin cell line. *Toxicology Letters*. 2010;199(2):193–200.
24. Anderson D, Yu TW, Phillips BJ, Schmerzer P. The effect of various antioxidants and other modifying agents on oxygen-radical generated DNA damage inhuman lymphocytes in the comet assay. *Mutat Res*. 1994;307:261–271.
25. Papis E, Rossi F, Raspanti M, et al. Engineered cobalt oxide nanoparticles readily enter cells. *Toxicol. Lett*. 2009;189:253–259.
26. Liu X, Qiu G, Li X. Shape-controlled synthesis and properties of uniform spinel cobalt oxide nanotubes. *Nanotechnology*. 2005;16:3035–3040.

27. Zou J, Chen Q, Jin X, et al. Olaquindox induces apoptosis through the mitochondrial pathway in HepG2 cells. *Toxicology*. 2011;285: 104–133.

28. Horev-Azaria L, Kirkpatrick CJ, Korenstein R, et al. Predictive toxicology of cobalt nanoparticles and ions: comparative in vitro study of different cellular models using methods of knowledge discovery from data. *Toxicol Sci*. 2011;122 (2):489–501.

29. Colognato R, Bonelli A, Bonacchi D, Baldi G, Migliore L. Analysis of cobalt ferrite nanoparticles induced genotoxicity on human peripheral lymphocytes: comparison of size and organic grafting-dependent effects. *Nanotox*. 2007;1(4):301–308.

30. Mahmoudi M, Simchi A, Milani AS, Stroeve P. Cell toxicity of super paramagnetic iron oxide nanoparticles. *J Colloid Interface Sci*. 2009;336:510–518.

31. Barillet S, Jugan ML, Laye M, et al. In vitro evaluation of SiC nanoparticles impact on A549 pulmonary cells: cyto-, genotoxicity and oxidative stress. *Toxicol Lett*. 2010;198:324–330.

32. Wise JP, Goodale BC, Wise SS. Silver nanospheres are cytotoxic and genotoxic to fish cells. *Aquat Toxicol*. 2010;97:34–41.

33. Ott M, Gogvadze V, Orrenius S, Zhivotovsky B. Mitochondria, oxidative stress and cell death. *Apoptosis*. 2007;12:913–922.

34. Rana SV. Metals and apoptosis: recent developments. *J Trace Elem Med Biol*. 2008;22:262–284.

35. Asharani PV, Mun GK, Hande MP, Valiyaveettil S. Cytotoxicity and genotoxicity of silver nanoparticles in human cells. *ACS Nano*. 2009;3: 279–290.

36. Janicke RU, Sprengart ML, Wati MR, Porter AG. Caspase-3 is required for DNA fragmentation and morphological changes associated with apoptosis. *J Biol Chem*. 1998;273:9357–9360.

37. Colognato R, Bonelli A, Ponti J, et al. Comparative genotoxicity of cobalt nanoparticles and ions on human peripheral leukocytes in vitro. *Mutagen*. 2008;23:377–382.

38. Petit A, Mwale F, Tkaczyk C, Antoniou J, Zukor DJ, Huk OL. Induction of protein oxidation by cobalt and chromium ions in human U937 macrophages. *Biomaterials*. 2005;26:4416–4422.

39. Shrivastava K, Shukla D, Bansal A, Sairam M, Banerjee PK, Ilavazhagan G. Neuroprotective effect of cobalt chloride on hypobaric hypoxia-induced oxidative stress. *Neurochem Int*. 2008;52:368–375.